

## Classification and prediction of frontotemporal dementia based on plasma microRNAs

Iddo Magen<sup>1</sup>, Nancy Sara Yacovzada<sup>1</sup>, Jason D. Warren<sup>2</sup>, Carolin Heller<sup>2,3</sup>, Imogen Swift<sup>2,3</sup>, Yoana Bobeva<sup>4</sup>, Andrea Malaspina<sup>4</sup>, Jonathan D. Rohrer<sup>2\*</sup> Pietro Fratta<sup>5\*</sup> and Eran Hornstein<sup>1\*</sup>

1 Department of Molecular Genetics, Weizmann Institute of Science, Rehovot, Israel

2 Dementia Research Centre, and 3 UK Dementia Research Institute, Department of Neurodegenerative Disease, UCL Queen Square Institute of Neurology, London, UK.

4 Centre for Neuroscience and Trauma, Blizard Institute, Barts and the London School of Medicine and Dentistry, Queen Mary University of London, London, UK.

5 Department of Neuromuscular Diseases, UCL Queen Square Institute of Neurology, London, UK

\* To whom correspondence should be addressed: [j.rohrer@ucl.ac.uk](mailto:j.rohrer@ucl.ac.uk); [p.fratta@ucl.ac.uk](mailto:p.fratta@ucl.ac.uk); [eran.hornstein@weizmann.ac.il](mailto:eran.hornstein@weizmann.ac.il);

Abstract word count: 242.

Text word count (excluding references and figure legends): 3528.

No. of items (figures, tables): 4, 2

References: 38

## 2 **Abstract**

3 Frontotemporal dementia (FTD) is a heterogeneous neurodegenerative disorder characterized by  
4 frontal and temporal lobe atrophy, typically manifesting with behavioural or language  
5 impairment. Because of its heterogeneity and lack of available diagnostic laboratory tests there  
6 can be a substantial delay in diagnosis. Cell-free, circulating, microRNAs are increasingly  
7 investigated as biomarkers for neurodegeneration, but their value in FTD is not yet established.  
8 In this study, we investigate microRNAs as biomarkers for FTD diagnosis. We performed next  
9 generation small RNA sequencing on cell-free plasma from 52 FTD cases and 21 controls. The  
10 analysis revealed the diagnostic importance of 20 circulating endogenous miRNAs in  
11 distinguishing FTD cases from controls. The study was repeated in an independent second cohort  
12 of 117 FTD cases and 35 controls. The combinatorial microRNA signature from the first cohort,  
13 precisely diagnosed FTD samples in a second cohort. To further increase the generalizability of  
14 the prediction, we implemented machine learning techniques in a merged dataset of the two  
15 cohorts, which resulted in a comparable or improved classification precision with a smaller panel  
16 of miRNA classifiers. In addition, there are intriguing molecular commonalities with cell free  
17 miRNA signature in ALS, a motor neuron disease that resides on a pathological continuum with  
18 FTD. However, the signature that describes the ALS-FTD spectrum is not shared with blood  
19 miRNA profiles of patients with multiple sclerosis. Thus, microRNAs are  
20 promising FTD biomarkers that might enable earlier detection of FTD and improve accurate  
21 identification of patients for clinical trials

## 23 **Introduction**

24 Frontotemporal dementia (FTD) is a clinically and neuroanatomically heterogeneous  
25 neurodegenerative disorder characterized by frontal and temporal lobe atrophy. It typically  
26 manifests between the ages of 50 and 70 with behavioral or language problems, and below the  
27 age of 65 is the second most common form of dementia, after Alzheimer's disease (1).

28  
29 Due to heterogeneity in clinical presentation FTD can be difficult to diagnose (2). Three main  
30 phenotypes are described: behavioral variant frontotemporal dementia (bvFTD), characterized by  
31 changes in social behaviour and conduct, semantic dementia (SD), characterized by the loss  
32 of semantic knowledge, leading to impaired word comprehension, and progressive non-fluent  
33 aphasia (PNFA), characterized by progressive difficulties in speech production (2, 3).

34  
35 FTD is also pathologically heterogeneous with inclusions seen containing hyperphosphorylated  
36 tau (4), TDP-43 (5), or fused in sarcoma (FUS) (6, 7). Mutations in the genes encoding for these  
37 proteins, as well as in other genes such as progranulin (GRN), chromosome 9 open reading  
38 frame 72 (C9ORF72), valosin-containing protein (VCP), TANK-binding kinase 1 (TBK1) and  
39 charged multivesicular body protein 2B (CHMP2B) are also associated with FTD (8-11).

40  
41 FTD overlaps clinically, pathologically and genetically with several other degenerative disorders.  
42 In particular, there is often overlap with amyotrophic lateral sclerosis (ALS): one in 5 ALS  
43 patients meets the clinical criteria for a concomitant diagnosis of FTD, and one in eight FTD  
44 patients is also diagnosed with ALS. TDP-43 inclusions are observed in the brains of both people

45 with FTD and ALS, and genetic evidence supports that these diseases reside along a continuum  
46 (5, 12-14).

47  
48 Previous studies have aimed to develop cell-free biomarkers for FTD, including TDP-43 (15),  
49 tau (16), and neurofilament light chain (NfL) (17), but none of these have shown use for  
50 diagnosis. microRNAs (miRNAs), endogenous non-coding RNAs, can be quantified in biofluids  
51 (18), and have been shown previously to be dysregulated in amyotrophic lateral sclerosis (ALS)  
52 and in FTD (19). Furthermore, they may be biomarkers of disease progression in other brain  
53 diseases, including ALS (20). Previous studies have assessed the initial potential of microRNAs  
54 as diagnostic FTD biomarkers including miRNA analysis in plasma (21, 22), CSF and serum  
55 (23), and CSF exosomes (24) but no definitive markers have so far been found. We therefore  
56 aimed to study a large cohort of patients with different clinical phenotypes and pathological  
57 forms of FTD, to see whether they are able to reliably distinguish cases from controls, and  
58 different forms of FTD from each other.

59  
60 Here, we provide an unbiased signature of plasma miRNAs that has good diagnostic power in a  
61 large and heterogeneous cohort of patients with FTD, which is further predictive in an  
62 independent second cohort and may contribute to FTD subtyping. Therefore, circulating  
63 miRNAs hold a fascinating potential as diagnostic biomarkers and as means for patient  
64 stratification in clinical trials.

65

66

67

## 68 **Results**

### 69 **A plasma miRNA classifier for FTD**

70 In order to characterize the potential of plasma miRNAs as biomarkers for FTD we assembled a  
71 cohort of 73 plasma samples (subject information in Table 1), purified RNA and performed next  
72 generation sequencing (NGS). As many as 2313 individual miRNA species were aligned to the  
73 human genome (GRCh37/hg19) across all samples. However, only 137 miRNA species  
74 exceeded a cut-off of  $\geq 100$  UMIs per sample averaged on all samples. Of the 137 detected  
75 miRNAs, 20 miRNA changed in a statistically significant manner in FTD plasma relative to  
76 control (p-value  $< 0.05$ , Wald test; Figure 1A). Two miRNAs, whose levels decreased to the  
77 greatest extent in FTD compared to controls, namely, miR-379-5p and miR-654-3p (1.4 fold),  
78 remained significant after multiple hypothesis testing (Figure 1B).

79  
80 We next studied miRNA capacity as binary disease classifiers, by generating receiver-operating  
81 characteristic (ROC) curves. ROC area under the curve (AUC) suggested modest predictive  
82 capacity for miR-379-5p and for miR-654-3p (AUC for both:  $0.71 \pm 0.07$ ,  $p < 0.01$ ; Figure 1C).

83  
84 We further utilized the combinatorial signature of the 20 miRNAs that were differentially  
85 expressed between FTD patient plasma and control (Table S1). Using these, an ROC AUC of  
86  $0.79 \pm 0.05$  ( $p < 0.0001$ , Fig. 1C) was found, which was superior to the prediction capacity of any  
87 individual miRNA.

88

89

## 90 **Assessment of plasma miRNA classifier for FTD in a second cohort**

91 We then performed a replication study in an independent cohort of 117 FTD cases and 35 age-  
92 matched controls (Table 1). In this study, the levels of 58 miRNAs decreased and 89 increased in  
93 a statistically significant manner in FTD, relative to control plasma (p-value <0.05, Wald test,  
94 Figure 2A and Table S1). Noticeable miRNAs were miR-125b-2-3p ( $\times 26$  up,  $p = 1.4 \times 10^{-25}$ ),  
95 miR-34b-5p ( $\times 23$  up, adj.  $p = 9.8 \times 10^{-23}$ ) and miR-379-5p ( $\times 2.2$  down,  $p = 1.9 \times 10^{-14}$ ). 144 of the  
96 147 miRNAs further survived adjustment for multiple comparisons by Benjamini–Hochberg  
97 procedure (adjusted p-value < 0.05).

98

99 The expression of the 20 miRNAs that were most differentially expressed in the first cohort  
100 correlated with their respective expression in the second cohort (Pearson R of log 2 fold-change  
101 = 0.75,  $p=0.0001$ , Fig. 2B). Furthermore, the combined predictive power of the 20 miRNAs, that  
102 were decided on as a classifier based on data of the first cohort, was slightly superior in the  
103 replication cohort, with an AUC of  $0.82 \pm 0.04$  ( $p < 0.0001$ , Fig. 2C).

104

105 In addition to external validation, by testing a second cohort, we sought to guarantee the  
106 generalizability by applying K-fold cross-validation, which is an internal validation technique to  
107 evaluate performance and prevent overfitting (25, 26). Towards this we divided the 225 datasets  
108 (from 56 control and 169 FTD samples) randomly into three equal parts, or ‘folds’, of 75  
109 datasets, each. A machine learning model was trained using each time 2 of the 3 data folds (150  
110 samples) for building a prediction model and applying the prediction rule to estimate the  
111 prediction precision on the remaining 75 samples in the remaining third fold. This step was  
112 repeated  $k = 3$  times iteratively so all folds were used twice in training and once for the testing

113 process. 136 miRNAs that were measured above noise levels in all cohorts were included,  
114 yielding the following AUCs: 0.90 for fold 1; 0.87 for fold 2; and 0.93 for fold 3, with an  
115 average AUC of 0.90 (Fig. 2D).

116  
117 We next aimed to reduce the complexity of the measurements required for prediction by  
118 identifying the top 20 miRNA predictors per fold, i.e. the 20 miRNAs with the highest weighted  
119 importance in predicting disease status (Fig. 3A-C). We reduced the number of miRNAs  
120 gradually, starting from a 43 miRNA panel composed of the top 20 predictors in at least one fold  
121 (i.e., in one, two or three folds), which resulted in AUCs of 0.87, 0.87, 0.94 and an average AUC  
122 of 0.89 (Fig. 3D). We then utilized 13 miRNAs that were among the top 20 in at least two folds  
123 which resulted in AUCs of 0.85, 0.89 and 0.93, and an average of 0.89 (Fig. 3E). Finally, we  
124 used only four miRNAs - miR-26a-5p, miR-326, miR-203a-3p and miR-629-5p – that were  
125 among the top 20 predictors in all three folds. Their combinatorial AUCs after cross-validation  
126 were 0.81, 0.83 and 0.89 and 0.85 on average (Fig. 3F). All panels of miRNAs used for the  
127 cross-validation are listed in Table S1.

128  
129 These measurements were comparable to the AUC obtained with 136 miRNAs (Fig. 2D),  
130 revealing that the diagnostic power was not compromised by a substantial reduction of the  
131 miRNA numbers.

132

133

134

135

## 136 **Overlap between FTD miRNA signature and ALS miRNA signature**

137 FTD and ALS are two diseases on a neuropathology continuum. We aimed to determine whether  
138 the miRNA signatures found in FTD and in ALS reveal any molecular similarity. For this  
139 purpose, we sequenced and analyzed the differences between 115 ALS cases and 103 controls  
140 (see Table 2). We also sequenced 17 samples from patients with multiple sclerosis (MS), because  
141 this disease is mechanistically different from FTD and involves autoimmune-related  
142 demyelination, so molecular similarity to FTD is not expected to be seen. 161 miRNA species  
143 were differentially expressed in either one of the diseases (FTD, ALS or MS) vs controls.  
144 Differentially expressed miRNAs in either FTD or ALS were correlated in fold-change values  
145 between the diseases (Pearson R for log-transformed values = 0.35,  $p < 0.0001$ , Figure 4A), but no  
146 such correlation was found between FTD and MS ( $R = -0.15$ ,  $p = 0.15$ , Figure 4B). Intriguingly,  
147 muscle-specific miR-206 robustly increases in ALS, in agreement with previous reports (27-30)  
148 with no change at all in FTD.

149  
150 We next tested the degree of overlap between miRNAs differentially expressed in FTD vs. ALS.  
151 Seven out of 20 miRNAs changed exclusively in FTD, and the remaining 13 miRNAs changed  
152 in a significant manner in both FTD and ALS (Figure 4C; Table S1). Remarkably, the  
153 directionality of change for these miRNAs (increase/decrease) was consistent across diseases for  
154 all of the miRNAs but one, miR-29a-3p which decreased in FTD and increased in ALS (Figure  
155 4A). Moreover, the fold-change values in this subset of 13 miRNAs that have changed in both  
156 ALS and FTD, were highly correlated between the diseases (Pearson R = 0.90,  $p < 0.0001$ ). In  
157 contrast, only five out of the 20 miRNAs that changed in FTD, also changed in MS (Figure 4D;  
158 Table S1). Taken together, the miRNA signature in FTD plasma shows a similarity to the ALS



159 plasma signature, but not to the MS signature, in accordance with pathological and clinical  
160 similarities between FTD and ALS.

161  
162 Finally, we employed the FTD predictor, based on 20 miRNAs that are changing in FTD on ALS  
163 and healthy control cohorts. The signature of 20 miRNAs was able to correctly call ALS from  
164 controls more than at random (ROC AUC = 0.63,  $p < 0.001$ , Table S2), while the seven miRNAs  
165 that are exclusively changed in FTD were not able to distinguish between ALS and control in a  
166 statistically significant manner (ROC AUC = 0.57,  $p = 0.06$ ). Thus, miRNAs that are differentially  
167 expressed in FTD have a moderate capacity to predict ALS.

168  
169 **miRNAs signature of FTD subtypes and FTD patients with different pathologies**

170 We next tested whether specific miRNAs changed in the main FTD subtypes, bvFTD, SD and  
171 PNFA. After statistical adjustment for multiple comparisons, four miRNAs decreased in a  
172 significant manner in PNFA, and two miRNAs decreased and one miRNA increased  
173 significantly in bvFTD, whereas the small SD sample numbers ( $n=8$ ) did not allow to depict  
174 microRNAs that are changed in a significant manner after adjustment for multiple comparisons  
175 (Fig. S1A-C).

176  
177 We calculated a decent combinatorial predictive power for the 20 miRNAs in distinguishing  
178 bvFTD / SD / PNFA from healthy controls: thus, for bvFTD vs. healthy controls in the original  
179 cohort we obtained an AUC of  $0.85 \pm 0.06$ ,  $p < 0.0001$ ; in the replication cohort AUC of  
180  $0.80 \pm 0.05$ ,  $p < 0.0001$ , Fig. S1D; for SD vs. controls, original cohort AUC was  $0.86 \pm 0.08$ ,

181 p=0.003; replication cohort AUC was  $0.79\pm 0.06$ ,  $p=0.0003$  (Fig. S1E); for PNFA vs. controls,  
182 original cohort AUC was  $0.81\pm 0.08$ ,  $p=0.002$ ; replication cohort AUC was  $0.81\pm 0.05$ ,  $p<0.0001$   
183 (Fig. S1F). We concluded that the combinatorial 20 miRNAs signature distinguishes FTD and its  
184 subtypes from controls with comparable AUCs, for all three subtypes.

185  
186 The overlap of symptoms between subtypes of FTD poses a diagnostic challenge (31). We  
187 therefore tested whether FTD subtypes could be distinguished based on miRNA signature. We  
188 analyzed miRNA differential expression of PNFA cases vs. non-PNFA, which pooled together  
189 bvFTD and SD cases, due to a similar molecular signature of SD and bvFTD. Fourteen miRNAs  
190 changed in a significant manner in PNFA vs non-PNFA: miR-625-3p, miR-625-5p, miR-126-5p,  
191 miR-146a-5p, miR-146b-5p, miR-340-5p, miR-181a-5p (all increased in PNFA compared to  
192 non-PNFA) and miR-342-3p, let-7d-3p, miR-122-5p, miR-192-5p, miR-16-5p, miR-203a-3p  
193 (decreased; Fig. S1G). The combinatorial signature of these fourteen miRNAs yielded an AUC  
194 of  $0.81\pm 0.08$  (Fig. S1H;  $p=0.0007$ ), indicating that PNFA can be differentiated from other types  
195 of FTD with a high accuracy.

196  
197 We also tested whether specific miRNAs changed between FTD cases with different likely  
198 underlying pathologies, i.e. tau and TDP-43. 19 FTD cases with predicted Tau pathology based  
199 on genetics (4 in cohort I + 15 in cohort II) were compared to 63 cases with predicted TDP-43  
200 pathology (23 in cohort I + 40 in cohort II). Fourteen miRNAs changed in a statistically  
201 significant manner, but none remained significant after correction for multiple hypotheses (Fig.  
202 S2A). The combinatorial signature of these 14 miRNAs had a weak classification power, though  
203 it was statistically significant (AUC of ROC =  $0.7\pm 0.06$ ,  $p=0.009$ , Fig. S2B). Taken together, the

204 miRNA profile in our dataset has limited diagnostic power for pathological subtypes of FTD, as  
205 opposed to FTD vs control and different clinical subtypes of FTD.

206

207

## 208 **Discussion**

209 Our study utilizes a large cohort of FTD blood samples. It is the first work that employs next  
210 generation sequencing technology for FTD biomarkers. We defined a signature, composed of 20  
211 miRNAs, that is able to classify FTD. This signature that was discovered in an initial cohort was  
212 informative when applied to a second cohort. These observations suggest that miRNAs can be  
213 potentially utilized in clinical sampling as diagnostic FTD markers, which is needed because of  
214 non-specific early symptoms and overlap with other degenerative and non-degenerative  
215 conditions. Ours is the largest cohort used for miRNA profile, and its use of unbiased exhaustive  
216 next generation sequencing can potentially explain the discrepancies from past studies with  
217 smaller cohorts and biased miRNA choices (21-24).

218 A classifier panel of 20 miRNAs had ~80% chance to correctly call FTD in the first cohort.  
219 Reassuringly, it was comparably informative in calling FTD correctly also on a second cohort. In  
220 addition to external (second cohort) validation, we applied machine learning to the whole dataset  
221 of 225 samples. Through iterative learning, we defined a signature created by 136 miRNAs that  
222 was able to call FTD correctly in 90% of cases. We then reduced the signature complexity to the  
223 usage of only 43 miRNAs with the highest classification power that kept a true FTD calling  
224 capacity of 90%. Toward clinical diagnostic usage it is warranted to test the predictor that was  
225 developed in machine learning on an independent cohort, preferentially of different ethnicity.

226

227 Interestingly, the miRNA signatures of FTD is akin of ALS perhaps reflecting on a shared patho-  
228 mechanism for these two neurodegenerative disorders on the ALS-FTD continuum. This  
229 similarity cannot be extended to multiple sclerosis, a disease that is driven by a different,

230 autoimmune, mechanism. Nonetheless, the two diseases are still two different entities and  
231 accordingly only 10% of the miRNAs that has changed in either disease were shared.

232

233 In summary, we have characterized a large FTD plasma cohort for miRNA expression by next  
234 generation sequencing and found specific patterns of changes that can contribute to diagnosis of  
235 FTD. These patterns seem to involve the ALS-FTD continuum, alluding to differences and  
236 commonalities in the underlying mechanisms that drive molecular changes in ALS and FTD.

237

238

## 239 **Materials and Methods**

### 240 **Standard protocol approvals, registrations, and patient consents**

241 Approvals were obtained from the local research ethics committee and all participants provided  
242 written consent (or gave verbal permission for a carer to sign on their behalf). For ALS samples,  
243 recruitment, sampling procedures and data collection have been performed according to Protocol  
244 (Protocol number 001, version 5.0 Final – 30th November 2015).

### 245 **Study design**

246 Based on power analysis, we found that about 20 control and 50 FTD samples are required to  
247 obtain an ROC of 0.7 with a power of 80% and a p-value of 0.05. We determined the sample size  
248 based on these calculations. Because sample processing was done in different batches, samples  
249 were randomly allocated to the batches and within each batch, the number of control and  
250 FTD/ALS/MS samples was balanced in order to reduce batch-associated bias.

### 251 **Participants and sampling**

252 Participants were enrolled in the longitudinal FTD cohort studies at UCL. Frozen plasma  
253 samples from the UCL FTD Biobank were shipped to the Weizmann Institute of Science for  
254 molecular analysis. Study cohort I: 52 FTD patients, 21 healthy controls. Study cohort II: 117  
255 FTD patients, 35 healthy controls. FTD patients were further assigned into two groups with  
256 predicted pathology of TDP-43 or tau, based on genetics and clinical phenotype. Patients  
257 positive for C9ORF72 repeats and progranulin (PRGN) mutations and/or presented with  
258 semantic dementia, were predicted to have TDP-43 pathology, while patients with MAPT  
259 mutations were predicted to have tau pathology. Demographic data are detailed in table 1.

260 ALS and MS samples and their respective healthy controls (N = 115, 17 and 103, respectively)  
261 were obtained from the ALS biomarker study. ALS patients were diagnosed according to

262 standard criteria by experienced ALS neurologists (32). Healthy controls were typically spouses  
263 or relatives of patients. Demographic data are detailed in table 2.

264 Plasma samples were stored in  $-80^{\circ}\text{C}$  until RNA extraction and subsequent small RNA next  
265 generation sequencing.

266

### 267 **Small RNA next generation sequencing**

268 Total RNA was extracted from plasma using the miRNeasy micro kit (Qiagen, Hilden, Germany)

269 and quantified with Qubit fluorometer using RNA broad range (BR) assay kit (Thermo Fisher

270 Scientific, Waltham, MA). For small RNA next generation sequencing (NGS), libraries were

271 prepared from 7.5 ng of total RNA using the QIAseq miRNA Library Kit and QIAseq miRNA

272 NGS 48 Index IL (Qiagen), by an experimenter who was blinded to the identity of samples.

273 Following 3' and 5' adapter ligation, small RNA was reverse transcribed, using unique

274 molecular identifier (UMI), primers of random 12-nucleotide sequences. This way, precise linear

275 quantification miRNA is achieved, overcoming potential PCR-induced biases (18). cDNA

276 libraries were amplified by PCR for 22 cycles, with a 3' primer that includes a 6-nucleotide

277 unique index. Following size selection and cleaning of libraries with magnetic beads, quality

278 control was performed by measuring library concentration with Qubit fluorometer using dsDNA

279 high sensitivity (HS) assay kit (Thermo Fisher Scientific, Waltham, MA) and confirming library

280 size with Tapestation D1000 (Agilent). Libraries with different indices were multiplexed and

281 sequenced on a single NextSeq 500/550 v2 flow cell (Illumina), with 75bp single read and 6bp

282 index read. Fastq files were demultiplexed using the User-friendly Transcriptome Analysis

283 Pipeline (UTAP) developed at the Weizmann Institute (33). Sequences were mapped to the

284 human genome using Qiagen GeneGlobe [analysis web tool](#).

285

## 286 **Statistical analysis and machine learning**

287 Plasma samples with  $\geq 40,000$  total miRNA UMIs were included. miRNA with average  
288 abundance of  $\geq 100$  UMIs per sample, across all samples, were considered above noise levels.  
289 miRNA NGS data was analyzed via DESeq2 package in R Project for Statistical Computing (34,  
290 35), under the assumption that miRNA counts followed negative binomial distribution and data  
291 were corrected for library preparation batch in order to reduce its potential bias. Ratio of  
292 normalized FTD counts to the normalized control counts presented after logarithmic  
293 transformation on base 2. *P* values were calculated by Wald test (35, 36) and adjusted for  
294 multiple testing according to Benjamini and Hochberg (37). For binary classification by  
295 miRNAs, receiver operating characteristic (ROC) curves for individual miRNAs or combinations  
296 of miRNAs were plotted based on voom transformation of gene expression data in R (38).  
297 Graphs were generated with GraphPad Prism 5.

298 Machine learning was performed on Python 3.6. Cohorts were merged and case-control number  
299 imbalance was mitigated by applying ADASYN algorithm ([https://imbalanced-](https://imbalanced-learn.readthedocs.io/en/stable/api.html)  
300 [learn.readthedocs.io/en/stable/api.html](https://imbalanced-learn.readthedocs.io/en/stable/api.html)), which simulates synthetic new healthy sample data from  
301 the existing data. Then, K-Fold cross validation was performed on the pooled data set with  $K=3$ .  
302 An ROC was generated for each of the three folds and individual and mean AUCs were  
303 calculated.

304

305



306 **Acknowledgements**

307 We thank Vittoria Lombardi (UCL) for technical assistance. We acknowledge patients with  
308 FTD, ALS, MS and healthy volunteers for their contribution and ALS biomarkers study co-  
309 workers for biobanking, which has made this study possible (REC 09/H0703/27). We also thank  
310 the the North Thames Local Research Network (LCRN) for its support. EH is the Mondry  
311 Family Professorial Chair and Head of the Nella and Leon Benozziyo Center for Neurological  
312 Diseases.

313

314 **Funding**

315 EH was supported by the ISF Legacy 828/17 grant, Target ALS 118945 grant, European  
316 Research Council under the European Union's Seventh Framework Programme (FP7/2007-2013)  
317 / ERC grant agreement n° 617351. Israel Science Foundation, the ALS-Therapy Alliance, AFM  
318 Telethon 20576 grant, Motor Neuron Disease Association (UK), The Thierry Latran Foundation  
319 for ALS research, ERA-Net for Research Programmes on Rare Diseases (FP7), A. Alfred  
320 Taubman through IsrALS, Yeda-Sela, Yeda-CEO, Israel Ministry of Trade and Industry, Y.  
321 Leon Benozziyo Institute for Molecular Medicine, Benozziyo Center Neurological Disease, Kekst  
322 Family Institute for Medical Genetics, David and Fela Shapell Family Center for Genetic  
323 Disorders Research, Crown Human Genome Center, Nathan, Shirley, Philip and Charlene Vener  
324 New Scientist Fund, Julius and Ray Charlestein Foundation, Fraida Foundation, Wolfson Family  
325 Charitable Trust, Adelis Foundation, MERCK (UK), Maria Halphen, Estates of Fannie Sherr,  
326 Lola Asseof, Lilly Fulop, E. and J. Moravitz. Teva Pharmaceutical Industries Ltd. as part of the  
327 Israeli National Network of Excellence in Neuroscience (NNE) postdoc Fellowship to IM  
328 117941. The Dementia Research Centre is supported by Alzheimer's Research UK, Brain

329 Research Trust, and The Wolfson Foundation. This work was supported by the NIHR Queen  
330 Square Dementia Biomedical Research Unit, the NIHR UCL/H Biomedical Research Centre and  
331 the Leonard Wolfson Experimental Neurology Centre (LWENC) Clinical Research Facility as  
332 well as an Alzheimer's Society grant (AS-PG-16-007). JDR is supported by an MRC Clinician  
333 Scientist Fellowship (MR/M008525/1) and has received funding from the NIHR Rare Disease  
334 Translational Research Collaboration (BRC149/NS/MH). PF is supported by an MRC/MND  
335 LEW Fellowship and by the NIHR UCLH BRC. This work was also supported by the Motor  
336 Neuron Disease Association (MNDA) 839-791

337

### 338 **Competing interests**

339 The authors state that they have no competing interests.

340

341 **References**

- 342 1. Harvey RJ, Skelton-Robinson M, and Rossor MN. The prevalence and causes of  
343 dementia in people under the age of 65 years. *J Neurol Neurosurg Psychiatry*. 2003;74(9):1206-  
344 9.
- 345 2. Rabinovici GD, and Miller BL. Frontotemporal lobar degeneration: epidemiology,  
346 pathophysiology, diagnosis and management. *CNS Drugs*. 2010;24(5):375-98.
- 347 3. Snowden JS, Neary D, and Mann DM. Frontotemporal dementia. *Br J Psychiatry*.  
348 2002;180:140-3.
- 349 4. Lee G, and Leegers CJ. Tau and tauopathies. *Prog Mol Biol Transl Sci*. 2012;107:263-93.
- 350 5. Neumann M, Sampathu DM, Kwong LK, Truax AC, Micsenyi MC, Chou TT, et al.  
351 Ubiquitinated TDP-43 in frontotemporal lobar degeneration and amyotrophic lateral sclerosis.  
352 *Science*. 2006;314(5796):130-3.
- 353 6. Neumann M, Rademakers R, Roeber S, Baker M, Kretschmar HA, and Mackenzie IR. A  
354 new subtype of frontotemporal lobar degeneration with FUS pathology. *Brain*. 2009;132(Pt  
355 11):2922-31.
- 356 7. Neumann M, Roeber S, Kretschmar HA, Rademakers R, Baker M, and Mackenzie IR.  
357 Abundant FUS-immunoreactive pathology in neuronal intermediate filament inclusion disease.  
358 *Acta Neuropathol*. 2009;118(5):605-16.
- 359 8. Fontana F, Siva K, and Denti MA. A network of RNA and protein interactions in Fronto  
360 Temporal Dementia. *Front Mol Neurosci*. 2015;8:9.
- 361 9. Sieben A, Van Langenhove T, Engelborghs S, Martin JJ, Boon P, Cras P, et al. The  
362 genetics and neuropathology of frontotemporal lobar degeneration. *Acta Neuropathol*.  
363 2012;124(3):353-72.
- 364 10. van Swieten J, and Spillantini MG. Hereditary frontotemporal dementia caused by Tau  
365 gene mutations. *Brain Pathol*. 2007;17(1):63-73.
- 366 11. Pottier C, Bieniek KF, Finch N, van de Vorst M, Baker M, Perkersen R, et al. Whole-  
367 genome sequencing reveals important role for TBK1 and OPTN mutations in frontotemporal  
368 lobar degeneration without motor neuron disease. *Acta Neuropathol*. 2015;130(1):77-92.
- 369 12. Majounie E, Renton AE, Mok K, Dopper EG, Waite A, Rollinson S, et al. Frequency of  
370 the C9orf72 hexanucleotide repeat expansion in patients with amyotrophic lateral sclerosis and  
371 frontotemporal dementia: a cross-sectional study. *Lancet Neurol*. 2012;11(4):323-30.
- 372 13. Renton AE, Majounie E, Waite A, Simon-Sanchez J, Rollinson S, Gibbs JR, et al. A  
373 hexanucleotide repeat expansion in C9ORF72 is the cause of chromosome 9p21-linked ALS-  
374 FTD. *Neuron*. 2011;72(2):257-68.
- 375 14. van Es MA, Hardiman O, Chio A, Al-Chalabi A, Pasterkamp RJ, Veldink JH, et al.  
376 Amyotrophic lateral sclerosis. *Lancet*. 2017;390(10107):2084-98.
- 377 15. Feneberg E, Gray E, Ansorge O, Talbot K, and Turner MR. Towards a TDP-43-Based  
378 Biomarker for ALS and FTLD. *Mol Neurobiol*. 2018;55(10):7789-801.
- 379 16. Meeter LHH, Vijverberg EG, Del Campo M, Rozemuller AJM, Donker Kaat L, de Jong  
380 FJ, et al. Clinical value of neurofilament and phospho-tau/tau ratio in the frontotemporal  
381 dementia spectrum. *Neurology*. 2018;90(14):e1231-e9.
- 382 17. Skillback T, Mattsson N, Blennow K, and Zetterberg H. Cerebrospinal fluid  
383 neurofilament light concentration in motor neuron disease and frontotemporal dementia predicts  
384 survival. *Amyotroph Lateral Scler Frontotemporal Degener*. 2017;18(5-6):397-403.

- 385 18. Coenen-Stass AML, Magen I, Brooks T, Ben-Dov IZ, Greensmith L, Hornstein E, et al.  
386 Evaluation of methodologies for microRNA biomarker detection by next generation sequencing.  
387 *RNA Biol.* 2018;15(8):1133-45.
- 388 19. Eitan C, and Hornstein E. Vulnerability of microRNA biogenesis in FTD-ALS. *Brain*  
389 *Res.* 2016.
- 390 20. Magen I, Coenen-Stass A, Malaspina A, Greensmith L, Lu CH, Fratta P, et al.  
391 Circulating miRNAs as prognostic and longitudinal markers for amyotrophic lateral sclerosis. In  
392 preparation.
- 393 21. Sheinerman KS, Toledo JB, Tsvinsky VG, Irwin D, Grossman M, Weintraub D, et al.  
394 Circulating brain-enriched microRNAs as novel biomarkers for detection and differentiation of  
395 neurodegenerative diseases. *Alzheimers Res Ther.* 2017;9(1):89.
- 396 22. Grasso M, Piscopo P, Talarico G, Ricci L, Crestini A, Tosto G, et al. Plasma microRNA  
397 profiling distinguishes patients with frontotemporal dementia from healthy subjects. *Neurobiol*  
398 *Aging.* 2019.
- 399 23. Denk J, Oberhauser F, Kornhuber J, Wiltfang J, Fassbender K, Schroeter ML, et al.  
400 Specific serum and CSF microRNA profiles distinguish sporadic behavioural variant of  
401 frontotemporal dementia compared with Alzheimer patients and cognitively healthy controls.  
402 *PLoS One.* 2018;13(5):e0197329.
- 403 24. Schneider R, McKeever P, Kim T, Graff C, van Swieten JC, Karydas A, et al.  
404 Downregulation of exosomal miR-204-5p and miR-632 as a biomarker for FTD: a GENFI study.  
405 *J Neurol Neurosurg Psychiatry.* 2018;89(8):851-8.
- 406 25. Al-Hameed S, Benaissa M, Christensen H, Mirheidari B, Blackburn D, and Reuber M. A  
407 new diagnostic approach for the identification of patients with neurodegenerative cognitive  
408 complaints. *PLoS One.* 2019;14(5):e0217388.
- 409 26. Baek S, Tsai CA, and Chen JJ. Development of biomarker classifiers from high-  
410 dimensional data. *Brief Bioinform.* 2009;10(5):537-46.
- 411 27. de Andrade HM, de Albuquerque M, Avansini SH, de SRC, Dogini DB, Nucci A, et al.  
412 MicroRNAs-424 and 206 are potential prognostic markers in spinal onset amyotrophic lateral  
413 sclerosis. *J Neurol Sci.* 2016;368:19-24.
- 414 28. Tasca E, Pegoraro V, Merico A, and Angelini C. Circulating microRNAs as biomarkers  
415 of muscle differentiation and atrophy in ALS. *Clin Neuropathol.* 2016;35(1):22-30.
- 416 29. Toivonen JM, Manzano R, Olivan S, Zaragoza P, Garcia-Redondo A, and Osta R.  
417 MicroRNA-206: a potential circulating biomarker candidate for amyotrophic lateral sclerosis.  
418 *PLoS One.* 2014;9(2):e89065.
- 419 30. Waller R, Goodall EF, Milo M, Cooper-Knock J, Da Costa M, Hobson E, et al. Serum  
420 miRNAs miR-206, 143-3p and 374b-5p as potential biomarkers for amyotrophic lateral sclerosis  
421 (ALS). *Neurobiol Aging.* 2017;55:123-31.
- 422 31. Hodges JR, and Piguet O. Progress and Challenges in Frontotemporal Dementia  
423 Research: A 20-Year Review. *J Alzheimers Dis.* 2018;62(3):1467-80.
- 424 32. Brooks BR, Miller RG, Swash M, Munsat TL, and World Federation of Neurology  
425 Research Group on Motor Neuron D. El Escorial revisited: revised criteria for the diagnosis of  
426 amyotrophic lateral sclerosis. *Amyotroph Lateral Scler Other Motor Neuron Disord.*  
427 2000;1(5):293-9.
- 428 33. Kohen R, Barlev J, Hornung G, Stelzer G, Feldmesser E, Kogan K, et al. UTAP: User-  
429 friendly Transcriptome Analysis Pipeline. *BMC bioinformatics.* 2019;24:154.

- 430 34. R Core Team. R: A Language and Environment for Statistical Computing. Vienna,  
431 Austria. *R Foundation for Statistical Computing* 2015.
- 432 35. Love MI, Huber W, and Anders S. Moderated estimation of fold change and dispersion  
433 for RNA-seq data with DESeq2. *Genome Biol.* 2014;15(12):550.
- 434 36. Anders S, and Huber W. Differential expression analysis for sequence count data.  
435 *Genome Biol.* 2010;11(10):R106.
- 436 37. Benjamini Y, Drai D, Elmer G, Kafkafi N, and Golani I. Controlling the false discovery  
437 rate in behavior genetics research. *Behav Brain Res.* 2001;125(1-2):279-84.
- 438 38. Law CW, Chen Y, Shi W, and Smyth GK. voom: Precision weights unlock linear model  
439 analysis tools for RNA-seq read counts. *Genome Biol.* 2014;15(2):R29.

440

441

Magen et al Table 1

442	Cohort I		Cohort II	
	Control	FTD	Control	FTD
Number of subjects (% males)	21 (62%)	52 (60%)	35 (51%)	117 (68%)
Age at enrolment	52±4 yr.	65±1 yr.	65±1 yr.	66±1 yr.
Age of onset (1 <sup>st</sup> reported symptoms)	N/A	61±1 yr.	N/A	60±1 yr.
Disease duration at enrolment	N/A	4.5±0.3 yr	N/A	6±0.3 yr
Clinical subtype (bvFTD/PNFA/SD/FTD-ALS/others)	N/A	25/15/8/2/2	N/A	57/25/20/3/12
Mutation carriers (C9ORF72/MAPT/ GRN/TBK1)	N/A	6/4/8/1	N/A	12/10/5/1
Likely pathology (TDP-43/Tau)	N/A	23/4	N/A	40/15

443 **Table 1.** Summary of demographic and clinical characteristics of FTD Cohorts I and II and  
444 control samples. bvFTD: behavioural FTD; PNFA: progressive nonfluent aphasia; SD: semantic  
445 dementia

446

447

448

449

450

451

452

453

454

455

456

457

458

459

460

Magen et al Table 2

	Controls	ALS	MS
Number of subjects (% males)	103 (27.2%)	115 (64.3%)	17 (29.4%)
Age at enrolment	52±2 yr.	64±1 yr.	57±2 yr.

462

463 **Table 2.** Summary of demographic and clinical characteristics of ALS, MS and control samples.  
464 ALSFRS-R: ALS functional rating scale. Demographic data recognizes that male ratio and age  
465 of first phlebotomy was significantly different between ALS cohort I and controls (proportion  
466 test:  $p < 0.0001$ ; t-test:  $p < 0.001$ , respectively).  
467

468

469

470

471

472

473

474

475

476

477

478

479

480

481

482

483

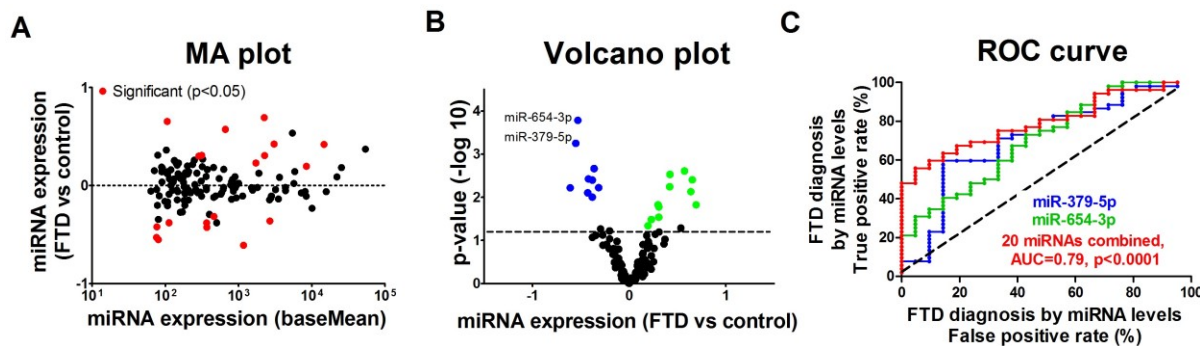
484

485

486

Magen et al Figure 1

488



489

490 **Figure 1. Predictive value of differential miRNA expression in FTD plasma.** (A) MA plot of  
491 differential miRNA expression in FTD (n=52) and heathy control (n=21 plasma samples). Log-2  
492 transformed fold-change, against the mean miRNA abundance. Red -significantly changed  
493 miRNAs (p-value  $\leq 0.05$ ). (B) A volcano plot of differentially expressed miRNAs between FTD  
494 (n=52) and heathy control (n=21 plasma samples). Each dot represents a single miRNA, plotted  
495 according to log 2 fold-change (FC) in FTD vs control (X-axis), and the negative log 10  
496 transformation of p-value (Y-axis). Black horizontal line demarcates  $p < 0.05$  and dots denote  
497 miRNAs with statistically significant differential expression in FTD plasma; green - increased in  
498 FTD; blue - decreased in FTD. (C) Receiver operating characteristic (ROC) curves demonstrate  
499 the capacity of miR-379-5p (blue, AUC=0.71,  $p=0.005$ ), miR-654-3p (green, AUC=0.71,  
500  $p=0.006$ ) and of a combinatorial signature of 20 miRNAs, whose differential expression is  
501 significant (red, AUC=0.79,  $p < 0.0001$ ; miRNAs listed in Table S1), to distinguish between FTD  
502 and healthy controls. True positive rate (sensitivity) as a function of the false positive rate (1-  
503 specificity) for different cut-off values. P-values are calculated given null hypothesis of area  
504 under the curve (AUC) =0.5.

505

506

507

508

509

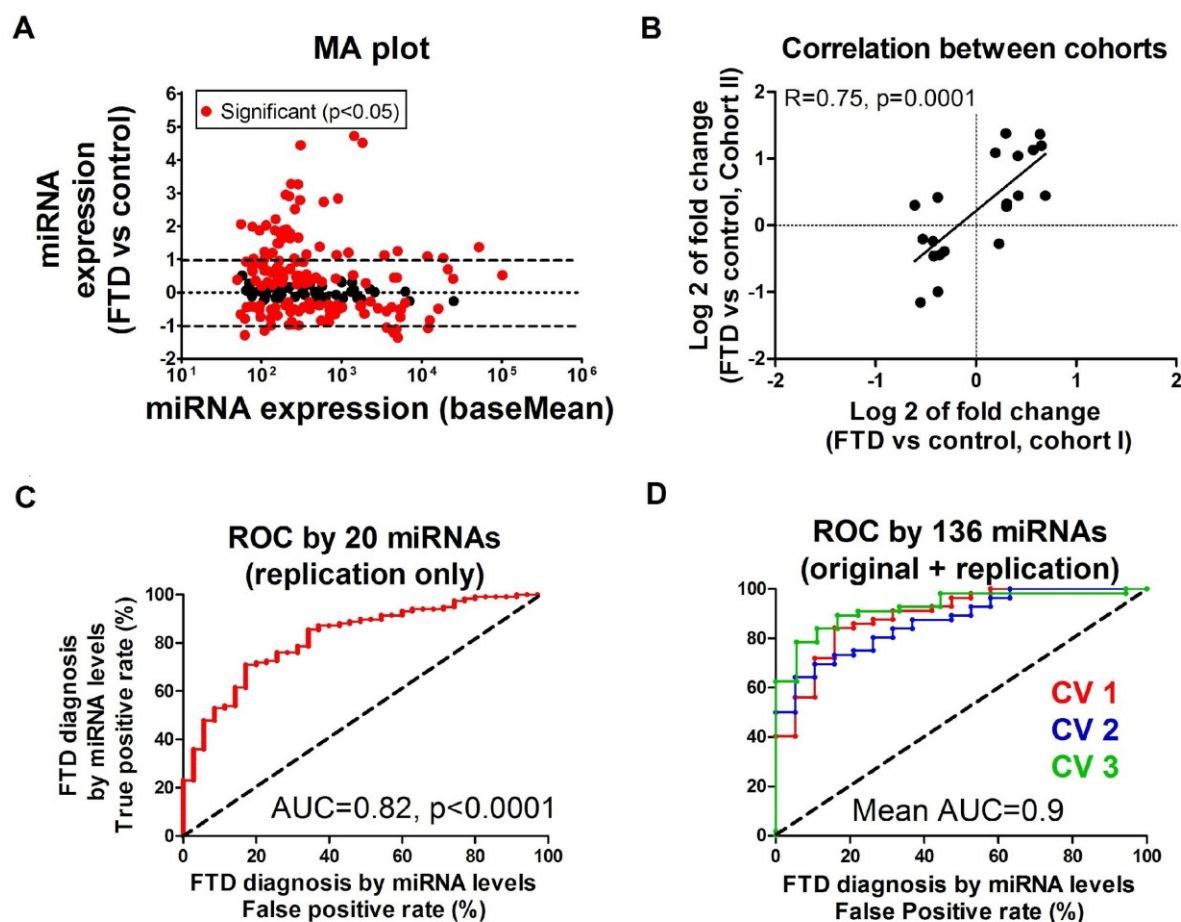
510

511

512



513  
Magen et al Figure 2  
514



515 **Figure 2. Replication of miRNA signature in a second cohort.** (A) MA plot of differential  
516 miRNA expression in a second cohort of FTD ( $n = 117$ ) and a second healthy control cohort ( $n = 35$   
517 plasma samples). Log-2 transformed fold-change, against the mean miRNA abundance. Red -  
518 significantly changed miRNAs ( $p$ -value  $\leq 0.05$ ). (B). Scatter plot of correlation between fold  
519 change of 20 miRNAs, which classify FTD, between the first and second cohorts. (C) ROC  
520 curve of a combinatorial signature of 20 miRNAs, whose differential expression is significant in  
521 the first cohort, distinguishes between FTD and healthy controls of the second cohort. True  
522 positive rate (sensitivity) as a function of the false positive rate (1-specificity) for different cut-  
523 off values. P-values are calculated given null hypothesis of area under the curve (AUC) = 0.5. (D)  
524 ROC curves based on K-fold cross validation with  $N = 3$  for a merged data set of 136 miRNA  
525 expression in both the discovery and the replication cohort (169 FTD cases and 56 healthy  
526 controls). Red, ROC for fold 1; blue, ROC for fold 2; green, ROC for fold 3.

527

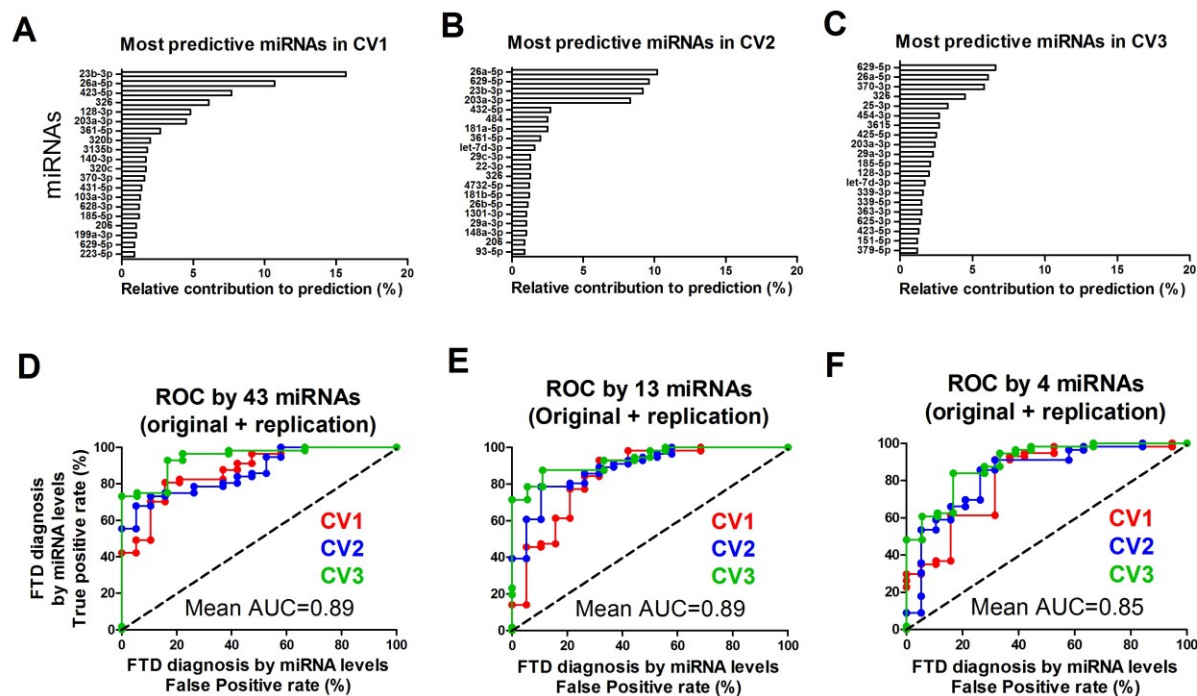
528

529

530

Magen et al Figure 3

532



533

534

535 **Figure 3. Most important miRNA classifiers in cross validation.** Top 20 miRNA classifiers in  
 536 (A) cross-validation fold 1 (B) fold 2 and (C) fold 3. (D-F) ROC curves based on K-fold cross  
 537 validation with N=3 for a merged data set including both the discovery and the replication cohort  
 538 (169 FTD cases and 56 healthy controls), when (D) only the 43 miRNAs depicted as "top 20" in  
 539 at least one fold (all of the miRNAs shown in panels A-C) are selected for classification. (E) 13  
 540 miRNAs depicted as "top 20" in at least two folds are selected and (F) only the four miRNAs  
 541 depicted as "top 20" in all three folds are selected. Red, ROC for fold 1; blue, ROC for fold 2;  
 542 green, ROC for fold 3.

543

544

545

546

547

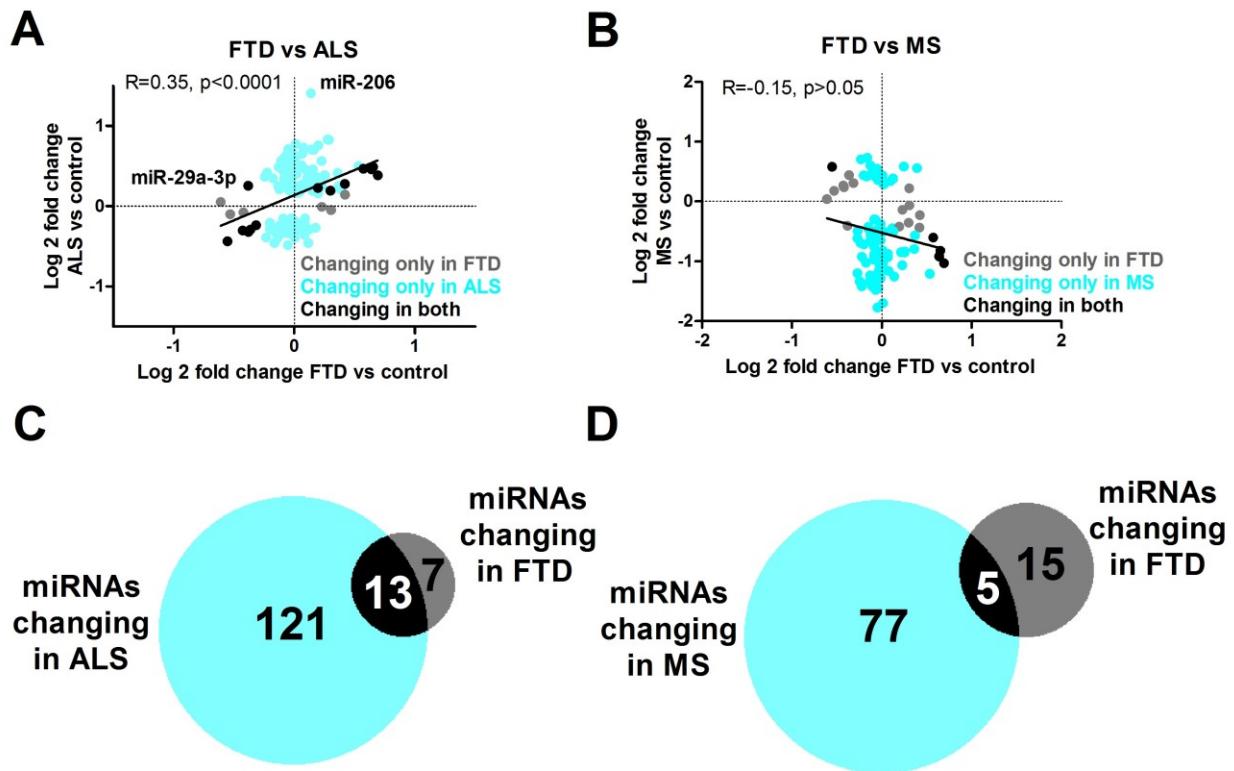
548

549

550

551

Magen et al Figure 4

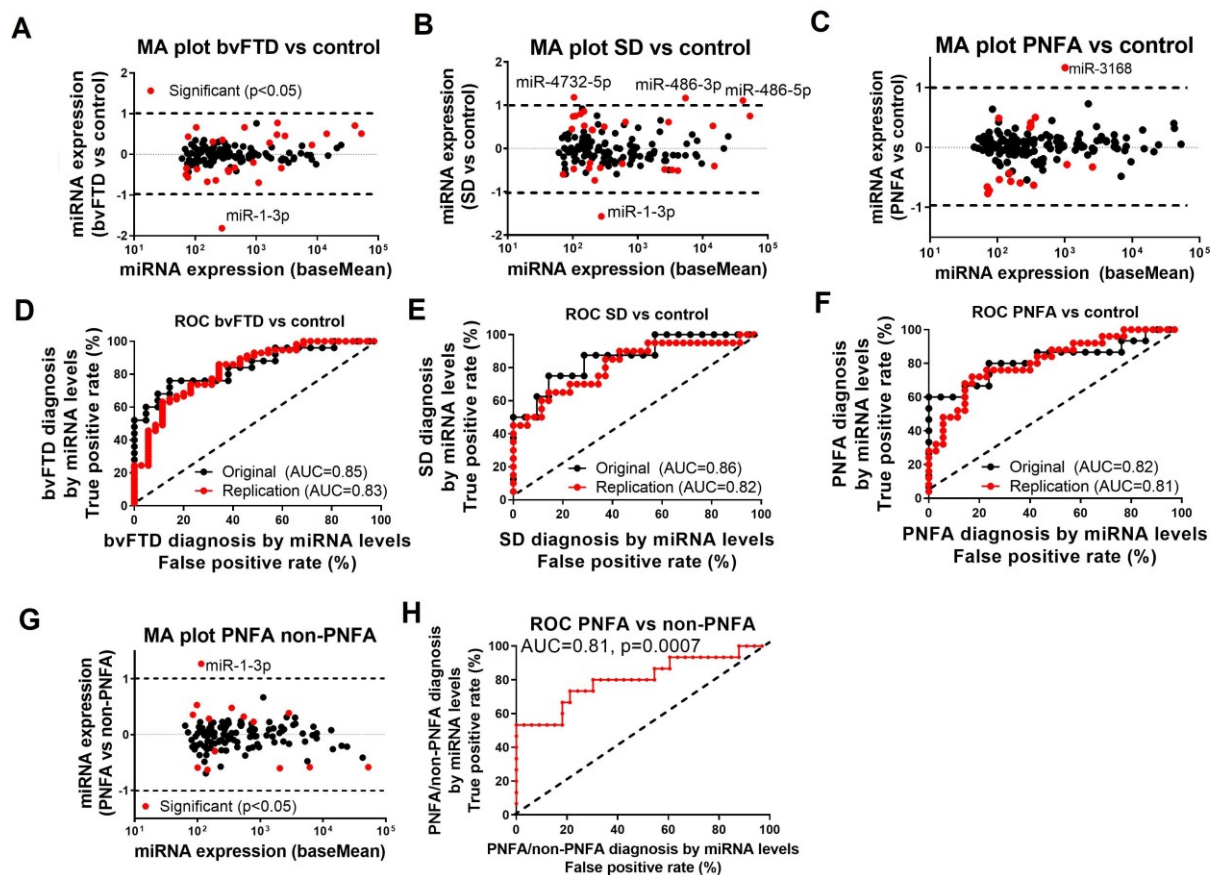


553 **Figure 4. Differential miRNA expression in ALS vs. FTD plasma.** (A) Scatter plot of  
554 correlation between ALS/control ratio and FTD/control ratio. (B) Scatter plot of correlation  
555 between MS/control ratio and FTD/control ratio. (C) Venn diagram of comparison between ALS  
556 and FTD with 13 shared miRNAs in the black portion. (D) Venn diagram of comparison between  
557 MS and FTD with 5 shared miRNAs in the black portion.

558

559 Supplementary figures

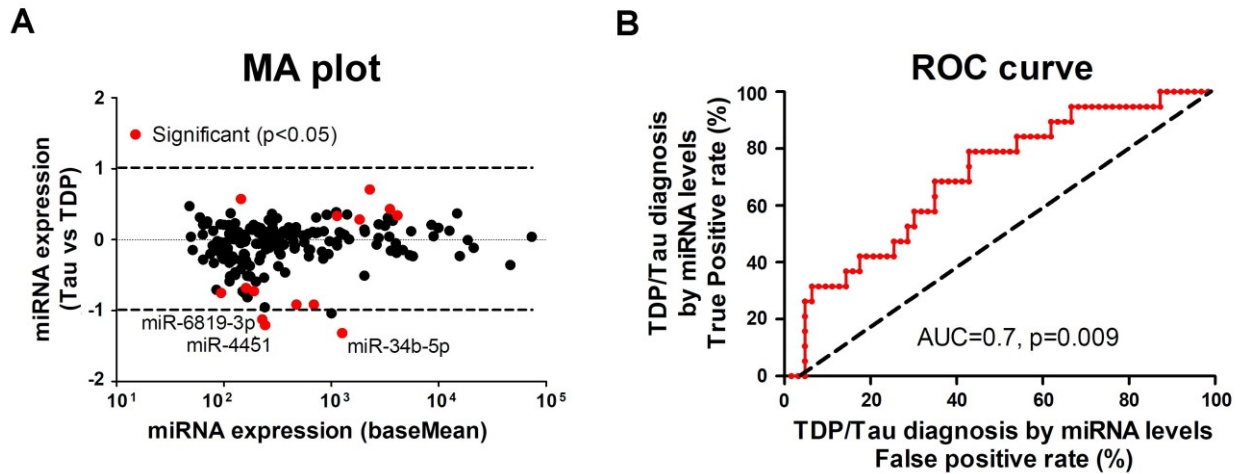
560



561 **Figure S1. miRNA profiles of FTD subtypes.** (A) MA plots of differential miRNA expression  
 562 in bvFTD patients (N=25), (B) SD patient (N=8) and (C) PNFA patients (N=15) compared to  
 563 healthy controls (N=21). Log-2 transformed fold-change, against mean miRNA abundance. Red  
 564 -significantly changed miRNAs (p-value  $\leq 0.05$ ). ROC curve of a combinatorial signature of 20  
 565 miRNAs, whose differential expression is significant in the first cohort, distinguishes (D)  
 566 bvFTD (E) SD and (F) PNFA from healthy controls, in the first (black) and second (red) studies. True  
 567 positive rate (sensitivity) as a function of the false positive rate (1-specificity) for different cut-  
 568 off values. P-values are calculated given null hypothesis of area under the curve (AUC) = 0.5.  
 569 (G) MA plot for differential miRNA expression between PNFA (N=15) and non-PNFA FTD  
 570 cases (bvFTD + SD (N=33)). Red- significantly changed miRNAs (p < 0.05). (H) ROC curve  
 571 based on combinatorial signature of 14 significant miRNAs for distinguishing PNFA and non-  
 572 PNFA FTD cases.

573

574



575 **Figure S2. miRNA profiles associated with FTD neuropathologies.** (A) MA plots of  
576 differential miRNA expression in FTD patients with predicted Tau pathology (N=19) vs patients  
577 with predicted TDP-43 pathology (N=63) from both cohorts used in the study. Log-2  
578 transformed fold-change, against mean miRNA abundance. Red -significantly changed miRNAs  
579 ( $p$ -value  $\leq 0.05$ ). (B) ROC curve based on combinatorial signature of 14 significant miRNAs for  
580 distinguishing FTD cases with Tau pathology from those with TDP-43 pathology.

581